Korean J. Chem. Eng., **30**(1), 50-54 (2013)
DOI: 10.1007/s11814-012-0094-0

Effect of nanocrystallite size of TiO_2 in Co/TiO_2 and Co/TiO_2-Ru catalysts on methanation

Kitima Pinkaew, Piyasan Praserthdam, and Bunjerd Jongsomjit†

Center of Excellence on Catalysis and Catalytic Reaction Engineering, Department of Chemical Engineering, Faculty of Engineering, Chulalongkorn University, Bangkok 10330, Thailand
(*Received 27 October 2011 • accepted 18 June 2012*)

Abstract−We studied the effect of crystallite size of nanocrystalline TiO_2 derived from the sol-gel method on the properties of Co/TiO_2 catalysts. First, nanocrystalline TiO_2 supports having different crystallite sizes were prepared via the sol-gel method by varying the water:alkoxide ratios from 4 to 165. Then, they were used as support for the cobalt catalyst. After calcination, the crystallite size of Co_3O_4 was dependent on the size of TiO_2 support. CO hydrogenation under methanation was performed to determine the activity and selectivity of Co/TiO_2 catalysts. It revealed that the catalyst with smaller size of TiO_2 crystallite exhibited higher catalytic activity due to higher Co dispersion without significant change in product selectivity. In addition, the Ru modification on the TiO_2 support was also investigated. The Ru modification resulted in increased activity regardless of the size of TiO_2 crystallite.

Key words: Nanocrystalline TiO_2, Sol-gel, Cobalt Catalyst, Methanation, CO Hydrogenation

INTRODUCTION

Fischer-Tropsch (FT) synthesis has been successfully used for future alternative resources instead of coal or crude oil. There are many active metals, such as Ru, Fe, Co, and Pd that can be used for hydrogenation of carbon monoxide (CO) to petroleum wax. For example, cobalt and iron are used for hydrocarbon synthesis. Even though the cobalt catalysts are more expensive, they are more resistant to deactivation than iron metals [1]. Supported cobalt catalysts have been extensively investigated with many inorganic supports for years, such as SiO_2 [2], Al_2O_3 [3], TiO_2 [4]. They have been the most popular FT catalysts for years due to their high catalytic activity and selectivity [5,6]. CO and H_2 (syngas) have been converted to paraffinic or long chain hydrocarbon through hydrogenation reaction. In fact, the interaction between cobalt oxide species and supports plays an important role in dispersion of cobalt oxide species [7]. The addition of small amount of noble metals apparently improves the catalytic properties [7-9]. For instance, the promotion with Ru in the supported cobalt catalysts also enhances the turnover rate and Co site density during reaction, as reported by Iglesia et al. [10].

Due to the significant developments in nanoscience and nanotechnology over recent years, many inorganic nanomaterials have been captivating the research in heterogeneous catalysis area. These inorganic nanomaterials can be potentially used as catalysts in some specified reactions, as supports for the catalytic phase, and also as nanofillers in composite materials. This can be attributed to their unique properties, great thermal and mechanical stability. In the present work, nanocrystalline TiO_2 having different crystallite sizes was prepared via the sol-gel method and used as the support for Co catalysts. In fact, the crystallite size of TiO_2 can be controlled by varying the water : alkoxide ratios during sol-gel synthesis. Thus, the effect of crystallite size of the TiO_2 support on the properties of Co catalysts can be elucidated. The characteristics of different supports and catalysts were determined by means of several techniques, such as XRD, SEM/EDX, TEM, TPR, CO chemisorption, and XPS. The activity and product selectivity of catalysts were measured via CO hydrogenation under methanation condition to minimize the catalyst deactivation.

†To whom correspondence should be addressed.
E-mail: bunjerd.j@chula.ac.th

EXPERIMENTAL

1. Preparation of Nanocrystalline TiO_2

TiO_2 was prepared by the sol-gel method [11,12]. First, the titania precursor [titanium (IV) isopropoxide] was dissolved in ethanol and then mixed with the solution of water:alkoxide, having molar ratios between 4 to 165 in order to obtain different crystallite sizes of TiO_2. The mixture was added dropwise to the aqueous solution with ultrasonic stirring at room temperature for 2 h. The obtained amorphous precipitates was centrifuged and redispersed in ethanol five times prior to filtration. After that, the sample was dried and calcined at 450 °C in air flow for 2 h.

2. Preparation of Ru-modified Nanocrystalline TiO_2

The Ru-modified TiO_2 support was prepared by the incipient wetness impregnation having 0.03 wt% of Ru. The desired amount of ruthenium (III) nitrosyl nitrate [$Ru(NO(NO_3)_3)$] was dissolved in deionized water, and then was dropped slowly to the TiO_2 support. The modified support was dried at 110 °C for 12 h and calcined in air at 500 °C for 4 h.

3. Preparation of Cobalt Catalysts

A 20 wt% of Co metal was impregnated onto the TiO_2 supports according to sections 1 and 2 using cobalt nitrate [$Co(NO_3)_2 \cdot 6H_2O$] as the precursor. The sample was dried at 110 °C for 12 h and calcined in air at 500 °C for 4 h to convert all cobalt nitrate precursors into Co oxide species [13].

The nomenclature used for the catalyst samples in this study is

as follows:

- Co/TiO_2_xx nm
- Co/TiO_2_xx nm_Ru

Co/TiO_2_xx nm refers to Co/TiO_2 catalyst with TiO_2 having the crystallite size of xx nm.

Co/TiO_2_xx nm_Ru refers to the Co/TiO_2 catalyst with TiO_2 having the crystallite size of xx nm with Ru modification on TiO_2 as mentioned in section 2.

4. Methanation

CO hydrogenation (H_2/CO=10/1) under methanation condition was performed to determine the overall activity of the samples. Hydrogenation of CO was carried out at 220 °C and 1 atm. A flow rate of H_2/CO/Ar=20/2/8 cm^3/min in a fixed-bed flow reactor was used. A relatively high H_2/CO ratio was used to minimize deactivation due to carbon deposition during reaction. Typically, 10 mg of a sample was reduced *in situ* in flowing H_2 (30 cm^3/min) at 350 °C for 10 h prior to the reaction. Reactor effluent samples were taken at 30-min intervals and analyzed by GC. Thermal conductivity detector (TCD) with molecular sieve 5A was used to detect the CO. A flame ionization detector (FID) with a VZ-10 column was used to detect the light hydrocarbons, such as C_1-C_4 hydrocarbons. In all cases, steady-state was reached within 5 h.

5. Characterization of Supports and Catalysts

5-1. N_2 Physisorption

The surface area was determined by physisorption of nitrogen (N_2) using a Micromeritics Pulse Chemisorb 2700 system. It was calculated based on nitrogen uptake at liquid-nitrogen temperature (77 K) using the Brunauer-Emmett-Teller (BET) equation by the single point method.

5-2. X-ray Diffraction

XRD was performed to determine the bulk crystalline phases of the sample. It was conducted using a SIEMENS D-5000 X-ray diffractometer with Cu K_α (λ=1.54439 Å). The spectra were scanned at a rate of 2.4°/min in the range 2θ=20-80°.

5-3. Scanning Electron Microscopy and Energy Dispersive X-ray Spectroscopy

SEM and EDX were used to determine the catalyst morphologies and elemental distribution throughout the sample granules, respectively. SEM involved a JEOLmodel JSM-5800LV. EDX was performed using Link Isis series 300 program.

5-4. Transmission Electron Microscopy

TEM was used to determine the dispersion of cobalt oxide species using JEOL-TEM 200CX transmission electron spectroscopy operated at 100 kV with 50 k magnification. The sample was dispersed in ethanol to obtain the uniform dispersion of sample prior to the measurement.

5-5. Temperature-programmed Reduction

TPR was used to determine the reduction behaviors of the samples. It was carried out using 50 mg of a sample and a temperature ramp from 35 to 800 °C at 5 °C/min. The carrier gas was 10% H_2 in Ar. A cold trap was placed before the detector to remove water produced during the reaction.

5-6. X-ray Photoelectron Spectroscopy

XPS was used to examine the binding energy and the surface composition of the catalysts by using an AMICUS spectrometer with X-ray source of Mg K_α radiation operated at voltage of 20 kV, current of 10 mA using the AMICUS "VISION2" software.

5-7. CO Chemisorption

The active sites and the relative percentages dispersion of cobalt catalyst were determined by CO-pulse chemisorption technique using Micromeritics ChemiSorb 2750 (pulse chemisorption system) and ASAP 2101C V.3.00 software. 20 mg of a sample was used and reduced in H_2 flow rate at 50 ml/min with heating from room temperature to 350 °C at rate 10 °C/min and held at this temperature for 3 h after being cooled to room temperature in He flow. Gas volumetric chemisorption at 100 °C was performed. Desorbed CO was measured with a thermal conductivity detector. Pulsing was continued until no further carbon monoxide adsorption was observed.

RESULTS AND DISCUSSION

1. Characteristics

First, the crystallite size of the sol-gel derived TiO_2 was varied by changing the water:alkoxide molar ratios (3 values from 4, 40, and 165) during the synthesis. In this sol-gel process, the reaction between the alkoxide precursor and the desired amount of water occurred in an anhydrous alcohol medium. The hydrolysis and condensation reactions can be summarized as follows [14]:

$$\text{Hydrolysis: } Ti(OC_3H_7)_4+4H_2O \rightarrow Ti(OH)_4+4C_3H_7OH \quad (1)$$

$$\text{Condensation: } Ti(OH)_4 \rightarrow TiO_2+2H_2O \quad (2)$$

$$\text{Net reaction: } Ti(OC_3H_7)_4+2H_2O \rightarrow TiO_2+4C_3H_7OH \quad (3)$$

As seen from the net reaction (3), the nucleation rate of TiO_2 increases with increasing the water:alkoxide ratios. As a result, the crystallite size and nanoparticle size should decrease with increasing the water:alkoxide ratios [15]. After calcination, the obtained TiO_2 supports were characterized using XRD and N_2 physisorption. All samples exhibited similar XRD patterns (not shown) at 26° (major), 37°, 48°, 55°, 56°, 62°, 69°, 71°, and 75° assigned to TiO_2 in the anatase phase. The crystallite sizes of TiO_2 were calculated based on the XRD line broadening using the Scherrer equation [16]. The crystallite sizes of TiO_2 were in the range of 11, 13 and 16 nm corresponding to the water:alkoxide ratios of 165, 40 and 4, respectively. It appeared that increased water:alkoxide molar ratio apparently resulted in decreased crystallite size of TiO_2 [14,15]. The BET surface areas of samples were found to be 71, 63 and 48 m^2/g for TiO_2_11 nm, TiO_2_13 nm, and TiO_2_16 nm, respectively, which is usual for anatase TiO_2 obtained from the sol-gel method. After Ru modification of the TiO_2 supports, it showed only a slight decrease in surface area. No XRD peaks of Ru were detected due to its highly dispersed form.

After impregnation of Co onto the different TiO_2 supports as mentioned above, the catalysts were calcined and characterized using various techniques. The XRD patterns for the calcined catalyst samples without Ru modification are shown in Fig. 1. Besides the appearance of XRD patterns of the anatase TiO_2 as mentioned above, all calcined samples exhibited XRD peaks at 31° (weak), 36° (strong), 46° (weak), and 65° (weak), which were assigned to the presence of Co_3O_4. Contrarily to Co/TiO_2_16 nm, XRD patterns of Co/TiO_2_11 nm and Co/TiO_2_13 nm both present a huge background. Such a background may originate from a larger water content that would be linked to the higher water:alkoxide ratio used for these catalysts or more probably from the poor crystallinity of TiO_2. However, no

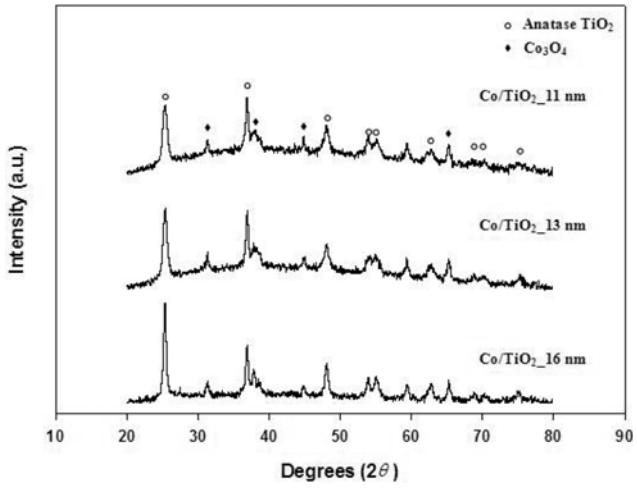

Fig. 1. XRD patterns for Co catalysts with different crystallite sizes of TiO_2 supports.

other forms of Co oxide species can be detected by XRD measurement. The XRD patterns for the calcined catalyst samples with Ru modification (not shown) were similar to those without Ru modification. The surface areas of the catalysts with and without Ru modification are shown in Table 1. They slightly decreased with Ru modification. It should be noted that high surface area could result in better distribution of Co, but somehow does not guarantee good dispersion as shown in our previous work [17]. The crystallite sizes of Co_3O_4 are also shown in Table 1. It indicated that the Ru modification can result in decreased crystallite size of Co_3O_4 on TiO_2 supports. To determine the Co dispersion and active sites, CO chemisorption was performed as also listed in Table 1. Apparently, the Co dispersion increased with Ru modification on the support. This phenomenon was in agreement with our previous work [6] when Ru was co-impregnated with cobalt onto the alumina support.

The morphologies and elemental distribution of the catalyst samples were determined by using SEM and EDX, respectively. The SEM micrographs for all catalyst samples are illustrated in Fig. 2. It can be seen that the larger crystallite sizes of TiO_2 support can result in more agglomeration of catalyst particles. The EDX mapping for all samples (not shown) also revealed good distribution of cobalt on the support granules. To determine the dispersion of cobalt oxide species on the different TiO_2 supports, a more powerful technique such as TEM was applied for all samples. The TEM micro-

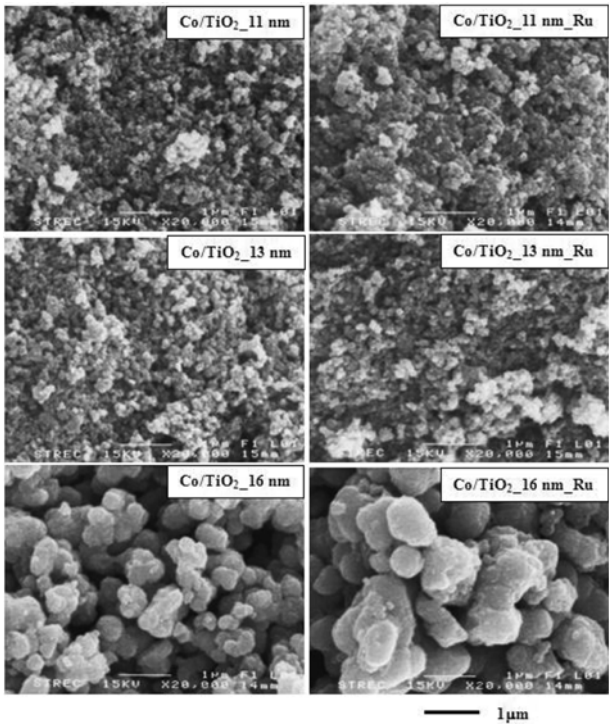

Fig. 2. SEM micrographs of Co catalysts with different crystallite sizes of TiO_2 supports with and without Ru modification.

graphs of all catalysts are shown in Fig. 3. The dark spots represent cobalt oxide species dispersed on the different TiO_2 supports. Based on TEM micrographs, the catalyst present on smaller size of TiO_2 crystallite exhibits better dispersion (seen as smaller patches) than the larger one. It is suggested that the dispersion of cobalt oxide species could be altered by size of the support, as mentioned in our previous work [18]. The Ru modification on TiO_2 supports shows a similar appearance to those without Ru modification. In addition, with the presence of the highly dispersed form of cobalt oxide species as seen for the smaller size of TiO_2 crystallite, the interaction of the cobalt oxides and support should be considered. Therefore, temperature-programmed reduction (TPR) on the calcined catalyst samples was performed to gain a better understanding according to such a reduction behavior.

The TPR profiles for all catalyst samples are shown in Fig. 4. The reduction of cobalt oxides to cobalt metal (Co^0) was observed

Table 1. Characteristics of catalyst samples

Samples	Surface area (m^2/g)	Crystallite size of Co_3O_4 (nm)[a]	CO chemisorption	
			CO chemisorption (μmole CO/g cat)	Co^0 dispersion[b] (%)
Co/TiO_2_11 nm	52	11	23.1	3.5
Co/TiO_2_11 nm_Ru	47	8.7	31.1	4.6
Co/TiO_2_13 nm	40	14.9	21.4	3.3
Co/TiO_2_13 nm_Ru	36	13.9	24.3	3.6
Co/TiO_2_16 nm	11	19.5	6.7	1.0
Co/TiO_2_16 nm_Ru	10	15.8	11.7	1.8

[a]Calculated based on XRD line broadening using Scherrer Equation

[b]Calculated based on fraction of Co^0 detected from CO chemisorption per Co^0 loading ×100

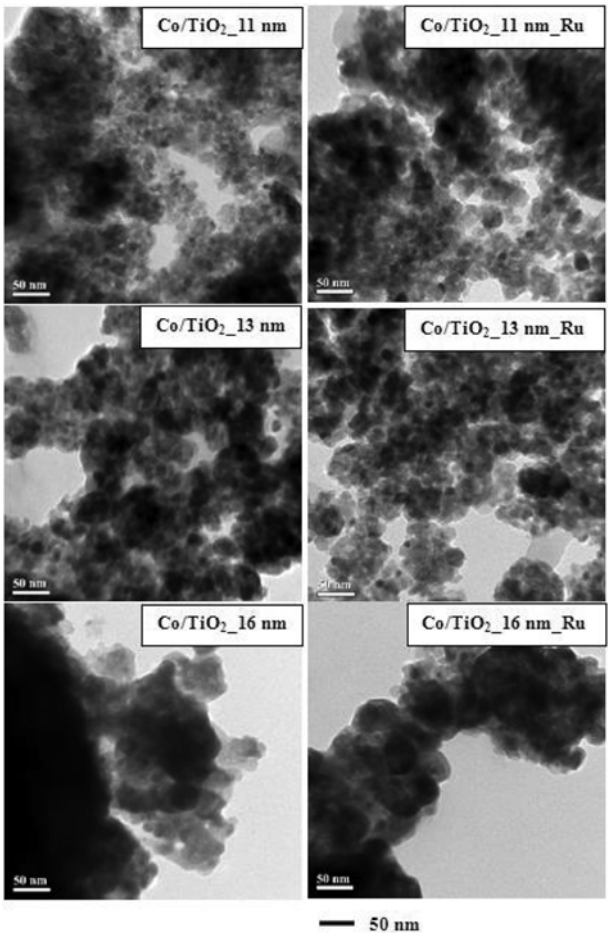

Fig. 3. TEM micrographs of Co catalysts with different crystallite sizes of TiO_2 supports with and without Ru modification.

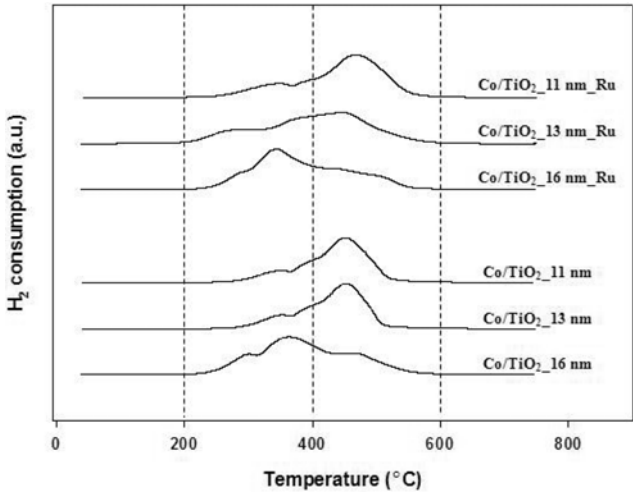

Fig. 4. TPR profiles of Co catalysts with different crystallite sizes of TiO_2 supports with and without Ru modification.

for all catalyst samples that occurred in a shoulder and one major peak. The lower reduction temperature shoulder peak of the unmodified catalysts was located at the 300 °C (for Co/TiO_2_16 nm) and 350 °C (for Co/TiO_2_11 and _13 nm). The broad peak was related to a two-step reduction of Co_3O_4 to CoO, and then to Co metal [5, 13,18]. The Co/TiO_2_16 nm sample exhibits broader TPR peaks compared to the others. This may be due to the presence of more various Co_xO_y species. With Ru modification, there is also one shoulder and one major peak for the catalysts with Ru modification located at 260 and between 350 and 460 °C. It appears that the broad peak is shifted to lower temperature with Ru modification. However, this phenomenon is not clearly seen for the Co/TiO_2_11 nm sample, suggesting that the Ru modification has less pronounced effect on the smaller crystallites. This indicates that Ru modification facilitates the reduction of Co catalysts. In some particular cases, the peak of the decomposition of the cobalt nitrates, as a cobalt precursor can be observed between 200 and 300 °C, especially on silica and alumina supports [6]. Prolonged calcination or reduction and recalcination resulted in complete decomposition of any cobalt nitrates present [6]. In addition, it has been often found that, due to interactions between Co_3O_4 and support materials, such as silica or alumina, the highest temperature peak represented the incomplete reduction of Co_xO_y-support. The TPR of supported Co_3O_4 can also manifest a separation of the two reduction steps [6,18-20]. A lower temperature shoulder between 200 and 350 °C peaks was observed due to some possible decomposition of residual Co nitrate. The reduction of Co_3O_4 to CoO and Co^0 occurred between 300 and 550 °C and can be assigned to the reduction of metal oxides on the support [6, 18-20]. The strong interaction between Co metal and support depends on the size of cobalt oxide species and nature of supports [6]. This suggested that the Ru may possibly help in the reduction of Co oxides and the support to make small crystallite size, which would decrease the Co^0 crystallite size. These results were in accordance with those reported by Hosseini et al. [21]. It was suggested that the use of Ru modified-TiO_2_11 nm and 13 nm supports can result in higher reduction temperature of Co oxides with larger amount of reducible cobalt oxide species.

XPS analysis was used to examine the binding energy and surface concentrations of species on the catalysts. The catalyst samples were analyzed in the Co 2p, Ti 2p, O 1s, Ru 3d with regards to the binding energy regions (not shown). The peaks of Ru 3d would be detected around 280 eV [22,23], but there was no observation of the Ru 3d due to very small amount of Ru loading. The binding energy values corresponding to Co 2p and Ti 2p were not affected by the small amount of Ru modification with the values of ca. 780 eV and 459.1 eV, respectively. These results are in accordance with those reported by Infantes-Molina et al. [22] and Reinikainen et al. [23].

2. Reaction Study

The reaction study was carried out via CO hydrogenation under methanation condition in order to minimize the catalyst deactivation due to carbon deposition. The conversion, reaction rate and product selectivity for all samples are shown in Table 2. The CO conversion ranged between 32 and 91% upon different crystallite sizes of TiO_2 supports. Based on the reaction rates, it is obvious that the activities of catalysts decreased with increasing the size of TiO_2 crystallite from 11 to 16 nm due to the decrease of Co dispersion. In addition, Ru modification apparently resulted in increased activity for all different crystallite sizes of TiO_2 supports. However, the Ru modification had more pronounced effect on the larger crystallite size support where the conversion increased about two times. This can be attributed to the promotion of cobalt dispersion by Ru because it can facilitate the reduction of cobalt oxide species [6]. It

Table 2. Reaction study

Samples	Conversion (%)	SS rate ($\times 10^2$ gCH_2/g cat·h)	Product selectivity (%)	
			C_1	C_2-C_4
Co/TiO_2_11 nm	77	28.9	97	3
Co/TiO_2_11 nm_Ru	91	34.1	97	3
Co/TiO_2_13 nm	49	18.4	94	6
Co/TiO_2_13 nm_Ru	89	33.4	99	1
Co/TiO_2_16 nm	32	12.0	94	6
Co/TiO_2_16 nm_Ru	77	28.9	99	1

is worth noting that Ru can be added into the Co catalyst as a promoter by coimpregnation with the cobalt precursor, such as cobalt nitrate. As a promoter for Co/Al_2O_3 catalysts [6], Ru increased both overall activity and reducibility. It was suggested that the Ru promoter not only facilitates the reduction of cobalt oxide at lower temperature, but also decreases the formation of Co strongly interacting with the alumina (Co_xO_y-Al_2O_3) and nonreducible Co aluminate by minimizing the impact of water vapor on this formation. However, for Ru promotion in Co/TiO_2 catalysts [24], it revealed that Ru promotion can only facilitate the reduction of cobalt oxide species, but has no effect on water vapor produced during reaction. Based on this study, it can be observed that the effects of Ru modification of TiO_2 supports are similar with those of Ru promotion as mentioned earlier. It is worth noting that with Ru modification, the effect of size of TiO_2 crystallite on Co/TiO_2 catalysts is less pronounced.

Considering the product selectivity, in all cases methane was present as a majority product, which is typical for CO hydrogenation under methanation. Without Ru modification, the catalysts having larger crystallite size of TiO_2 trended to give greater amounts of longer chain hydrocarbons (C_2-C_4). However, the C_1-C_4 decreased with the Ru promotion. It is known that CO hydrogenation is a kind of polymerization reaction where insertion of the -CH_2- (methylene group) occurs through the active centers [25], rate of propagation, and rate of termination. Obviously, a termination of chain growth occurs and is recognized as the chain growth probability. Based on product selectivity as found here, it can be concluded that the Ru modification in TiO_2 supports slightly inhibited the chain growth probability. As a matter of fact, it resulted in the observation of higher methane selectivity with Ru modification.

CONCLUSIONS

Based on this study, the effect of different crystallite sizes of TiO_2 supports on the catalytic properties of Co/TiO_2 catalysts can be elucidated. The smaller crystallite size of TiO_2 support exhibited higher catalytic activity due to higher Co dispersion. The crystallite sizes of cobalt oxide species were replicated by those of the TiO_2 support. It also revealed that the Ru modification on the support apparently increased the activity of catalysts as seen when Ru was used as a promoter by coimpregnation with the cobalt precursor. However, with the Ru modification, the effect of size of TiO_2 crystallite on Co/TiO_2 catalyst was less pronounced. The Ru promotion can result in slightly decreased C_2-C_4 hydrocarbons during methanation.

ACKNOWLEDGEMENT

The authors thank the Thailand Research Fund (TRF) and Office of the Higher Education Commission (CHE) for the financial support of this project.

REFERENCES

1. A. Y. Khodakov, W. Chu and P. Fongarland, *Chem. Rev.*, **107**, 1692 (2007).
2. K. Okabe, X. Li, M. Wei and H. Arakawa, *Catal. Today*, **89**, 431 (2004).
3. A. Kogelbauer, J. G. Goodwin, Jr. and R. Oukaci, *J. Catal*., **160**, 125 (1996).
4. S. J. Tauster, S. C. Fung and R. L. Garten, *J. Am. Chem. Soc*., **100**, 170 (1978).
5. B. Jongsomjit and J. G. Goodwin, Jr., *Catal. Today*, **77**, 191 (2002).
6. B. Jongsomjit, J. Panpranot and J. G. Goodwin Jr., *J. Catal.*, **204**, 98 (2001).
7. S. L. Soleda, E. Iglesia, R. A. Fiatoa, J. E. Baumgartnera, H. Vromana and S. Miseoa, *Topics Catal.*, **26**, 101 (2003).
8. N. Tsubaki, S. Sun and K. Fujimoto, *J. Catal.*, **199**, 236 (2001).
9. G. Jacobs, T. K. Das, Y. Zhang, J. Li, G. Racoillet and B. H. Davis, *Appl. Catal. A: Gen*., **233**, 263 (2002).
10. E. Iglesia, S. L. Soled, R. A. Fiato and G. H. Via, *J. Catal.*, **143**, 345 (1993).
11. K. Suriye, P. Praserthdam and B. Jongsomjit, *Appl. Surf. Sci.*, **253**, 3849 (2007).
12. K. Suriye, P. Praserthdam and B. Jongsomjit, *Ind. Eng. Chem. Res*., **44**, 6599 (2005).
13. B. Jongsomjit, C. Sakdamnuson, J. G. Goodwin Jr. and P. Praserthdam, *Catal. Lett*., **94**, 209 (2004).
14. S. Shukla, S. Seal and R. Vanfleet, *J. Sol-Gel Sci. Technol*., **27**, 119 (2003).
15. K. V. Baiju, S. Shukla, K. S. Sandhya, J. James and K. G. K. Warrier, *J. Phys. Chem. C*, **111**, 7612 (2007).
16. L. E. Alexander, *X-ray diffraction procedures for polycrystalline amorphous*, 2nd Ed., Wiley & Sons, New York (1974).
17. B. Jongsomjit, T. Wongsalee and P. Praserthdam, *Mater. Chem. Phys.*, **97**, 343 (2006).
18. S. Kittiruangrayab, T. Burakorn, B. Jongsomjit and P. Praserthdam, *Catal. Lett.*, **124**, 376 (2008).
19. A. Kogelbauer, J. G. Goodwin, Jr. and R. Oukaci, *J. Catal.*, **160**, 125 (1996).
20. J. Li, G. Jacobs, Y. Zhang, T. Das and B. H. Davis, *Appl. Catal. A: Gen.*, **223**, 195 (2002).
21. S. A. Hosseini, A. Taeb, F. Feyzi and F. Yaripour, *Catal. Commun*., **5**, 137 (2004).
22. A. Infantes-Molina, J. M. Rida-Robles, E. R. Guez-Castello, J. L. G. Fierro and A. J. Nez-Lopez, *Appl. Catal. A: Gen*., **341**, 35 (2008).
23. M. Reinikainen, M. K. Niemela, N. Kakuta and S. Suhonen, *Appl. Catal. A: Gen.*, **174**, 61 (1998).
24. B. Jongsomjit, C. Sakdamnuson, J. Panpranot and P. Praserthdam, *React. Kinet. Catal. Lett.*, **88**, 65 (2006).
25. B. Jongsomjit S. Kittiruangrayub and P. Praserthdam, *Mater. Chem. Phys.*, **105**, 14 (2007).